INTERNATIONAL JOURNAL FOR NUMERICAL METHODS IN BIOMEDICAL ENGINEERING
Int. J. Numer. Meth. Biomed. Engng. 0000; **00**:1–25
Published online in Wiley InterScience (www.interscience.wiley.com). DOI: 10.1002/cnm

Computational model of collagen turnover in carotid arteries during hypertension

P. Sáez[†] [*],E. Peña[*],J.M. Tarbell[‡],M.A. Martínez[*]

[†]*Mathematical Institute,University of Oxford, Oxford, UK*
[*]*Group of Group of Applied Mechanics and Bioengineering. Aragón Institute of Engineering Research. University of Zaragoza. CIBER-BBN. Centro de Investigación Biomédica en Red en Bioingeniería, Biomateriales y Nanomedicina.*
[‡]*Department of Biomedical Engineering, The City College of CUNY, New York, NY, USA*

SUMMARY

It is well known that biological tissues adapt their properties due to different mechanical and chemical stimuli. The goal of this work is the study of the collagen turnover in the arterial tissue of hypertensive patients through a coupled computational mechano-chemical model. Although it has been widely studied experimentally, computational models dealing with the mechano-chemical approach are not. The present approach can be extended easily to study other aspects of bone remodeling or collagen degradation in heart diseases. The model can be divided into three different stages. First, we study the smooth muscle cell synthesis of different biological substances due to the over-stretching during hypertension. Next, we study the mass-transport of these substances along the arterial wall. The last step is to compute the turnover of collagen based on the amount of these substances in the arterial wall which interact with each other to modify the turnover rate of collagen. We simulate this process in a finite element model of a real human carotid artery. The final results show the well known stiffening of the arterial wall due to the increase in the collagen content.

Received . . .

KEY WORDS: Collagen turnover; Hypertension; Soft tissue; FEM

1. INTRODUCTION

Hypertension is a very common medical condition in which the blood pressure increases. In the case of essential hypertension, this is due to the increased resistance to blood flow in the peripheral vasculature. There are several consequences for hypertensive patients, in particular, regarding the arterial tissue. The $thickening$ of the arterial wall has been widely documented [Owens, 1989, Owens et al., 1981, Saez et al., 2012b]. Endothelial cells are known to react to changes in the blood flow and to hypertensive conditions [Brunner et al., 2005, Li et al., 2005, Feihl et al., 2008] converting mechanical stimuli into intracellular signals that, e.g., release Nitric Oxide (NO). NO is known to have an important role in the vasodilating mechanism and the formation of atheroma plaque Pritchard et al. [1995]. Furthermore, the arterial tissue undergoes an increase in the density of collagen fibers, $stiffening$, due to unbalance of biochemical substances. Therefore, the arterial tissue stiffens hence reducing the compliance of the vessel. Collagen is a fundamental component of many biological tissues, arteries in particular. A large number of *in-vitro* and *in-vivo* experiments have shown the influence of different types mechanical loads in Smooth Muscle Cells (SMC) [Sumpio et al., 1988, Gupta and Grande-Allen, 2006, Dabagh et al., 2008] and in TGF-β

[*]Correspondence to: saez@maths.ox.ac.uk

turnover [Bishop et al., 1998, Butt and Bishop, 1997, O'Callaghan and Williams, 2000, Strauss and Rabinovitch, 2000]. There are also computational models of collagen remodeling [Driessen et al., 2003, Kuhl et al., 2005, Nagel] and collagen turnover, e.g,. [Boerboom et al., 2003] in the cardiovascular tissue.

In terms of collagen deposition fibrogenic cytokine proteins such as the transforming growth factor **TGF-β** are the most important regulators of collagen synthesis (see e.g. Border and Noble [1994], Wrana et al. [1994]) by vascular fibroblasts [Burke and Ross, 1979, Roberts et al., 1986]. TGF-β is a protein that influences cellular functions such as proliferation or differentiation and plays a key role in numerous cardiovascular diseases [Massague et al., 2000] and cancer [Massague, 2008]. The activation pathway [Massague, 2000] of the TGF-β family, which is part of a superfamily of proteins, is still not completely understood. It also plays a prominent role in the SMC proliferation [Owens, 1995, Raines, 2004]. Butt et al. [1995] reported the SMC release TGF-β growth factor associated with an increase in procollagen deposition and a decrease in collagen degradation. They also showed that both SMC and endothelial cells are the sources of the platelet-derived growth factor PDGF, an other important growth factors. The molecular structure of TGF-β has a molecular weight of 25 [kDa] and an equivalent external radius of around $3.8 \cdot 10^{-9}$[m]. These features are important for the diffusion and convection phenomenon.

Matrix metalloproteinase (MMP) [Nagase and Woessner, 1999] and **Tissue Inhibitors of Metalloproteinase** (TIMP) [WojtowiczPraga et al., 1997] could be the most important substance for quantifying the evolution of collagen degradation [Galis and Khatri, 2002]. MMP [Galis et al., 1994], in addition to other regulatory mechanisms such as cell differentiation and apoptosis, is responsible for extracellular matrix (ECM) degradation in general, and for collagen degradation in particular. TIMPs are a type of inhibitor of metalloproteinase. In hypertension, TIMP has been reported to increase, decreasing the total MMP-1 which in turn decreases the rate of collagen degradation. O'Callaghan and Williams [2000] have shown that the amount of collagen turnover increases with the magnitude of the strain imposed on SMC in *in-vitro* experiments. They also reported the production of MMP-2, a gelatinase-degrading enzyme and TGF-β (see also Sarzani et al. [1989], Hamet et al. [1991]), which could be stimulated by cyclic stretching. TIMP acts as an important regulator of ECM production, mainly by inhibition of MMP-1 and by increasing the activity of MMP-2. The MMP-1 activity is blunted by an increase of TIMP-1 which subsequently leads to a net increase of collagen content [Stakos et al., 2010]. Other studies have shown different aspects. For example, McNulty et al. [2006] have shown that increased MMPs levels and that the subsequent digestion of collagen type-I gives space to the accumulation of collagen type-III which, in turn, increase the stiffness of the tissue. Accumulation of collagen type I is associated with the increase of stiffness as a response of an increasing pressure load while collagen type-III is more related with the extensibility of the arterial wall [Bishop and Lindahl, 1999, Chamiot Clerc et al., 1999]. This newly and thicker syntethized collagen fibers requires the native collagen to be digested by MMPs [Tan et al., 2007, Yasmin et al., 2005, Flamant et al., 2007]. The molecular structure of MMP-1 and TIMP-1 has a molecular weight of 52 [kDa] and 28 [kDa] respectively and an equivalent external radius of around $4 \cdot 10^{-9}$[m] and $7 \cdot 10^{-9}$[m], respectively. MMP-1 is known as one of the most important collagenases. In short, stretching of the SMC promotes the synthesizing of TGF-β and also the activation and secretion of TIMPs. TIMPs make the overall MMPs in the tissue to decrease. The decreases of MMPs together with the increase of TGF-β makes the overall amount of collagen to increase in the tissue.

Mass transport phenomena, the movement of particles or molecules, have been studied for a long time. The pioneering works by Fick [1855], concerning diffusion phenomena (see, e.g. Philibert [2006] for a review), by Einstein [1905] about Brownian motion those related to atomistic and macroscopic transport (see e.g. Maxwell [1871], Huang [1987]) initiated a considerable number of studies relating to mass transport. Mass transport toward and within the arterial wall is a fundamental process for understanding not only different vascular diseases but also the normal evolution of arteries. Mass transport of different kinds of molecules in arterial tissue occurs due to concentrations and pressure gradients across the thickness by well known diffusion and convective phenomena [Tarbell, 2003, Dabagh et al., 2009a]. Low-density proteins (LDL) are probably the most

DOI: 10.1002/cnm

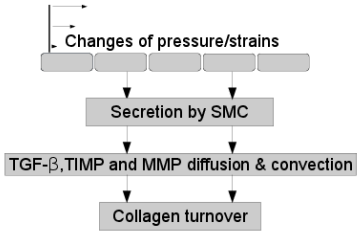

Figure 1. Flowchart of the steps followed in the model.

extensively studied form of molecular transport since they are the main initiator of atheroesclerotic plaque [Lusis, 2000, Maher, 2011]. Many experimental and numerical studies have appeared on this subject in recent years, e.g. Curmi et al. [1990], Glagov et al. [1988], Cancel et al. [2007] and Kim and Tarbell [1994], Huang and Tarbell [1997], Tada and Tarbell [2002], Dabagh et al. [2009b] for experimental and numerical works respectively. There are, however, other important molecules involved in hypertension that gain less attention but also play an important role in the collagen turnover. As discussed above, in this work we examine three substances: TGF-β, TIMP-1 and MMP-1. In the next section we study how these three molecules move through the arterial wall according to their specific features.

In this work, we study the mass production of different substances of interest within the context of collagen turnover in arterial tissue. Classical closed-systems in continuum mechanics keep mass changes constant. However, this is not usually the case with biological tissues. For this reason we consider the thermodynamic theory of open systems in this study. This assumes a non-vanishing term, called the source term $\mathcal{R}$ which fulfills mass balance equation. Then we discuss some particular substances and processes of interest in hypertensive disease. After that we study the mass transport phenomena through the arterial wall. Finally, we consider the production of collagen by fibroblast, which we directly relate with the amount of TGF-β and the collagen degradation, based on the amount of MMP-1 in the tissue. Both deposition and degradation can occur at the intracellular (collagen molecules) or extracellular (tropocollagen) levels.

2. METHODS

In this section, we first discuss the mechanical model for arterial tissue and for human carotid arteries in particular. Based on this mechanical behavior and the changes of pressure we define a model of mass production which is based on the the stretch ratio between the normotensive and hypertensive states. The SMC secrete difference substances that are transported by convective and diffusion phenomena throughout the artery. Finally, we define a collagen turnover model based on the amount the previously secreted substances. This flowchart is depicted in Fig. 1.

2.1. Mechanical model of carotid artery.

In this first part we present the basic notions of the mechanical problem. Our later approaches make use of the over-stretch of the SMC and therefore the constitutive relations have to be provided. Our model is based on a classical quasi-incompressible anisotropic hyperelastic formulation.

We start by defining some notions of kinematics. The tangent of the motion φ, the deformation gradient, represents a two-point linear map over the reference configuration, defined as $\mathbf{F} = \nabla_{\boldsymbol{X}} \boldsymbol{\varphi}$. The Jacobians of the deformation gradient will be denoted as $J = \det(\mathbf{F})$. We can then introduce the right Cauchy Green tensor $\mathbf{C} = \mathbf{F}^{\mathrm{t}} \cdot \mathbf{F}$.

The quasi-incompressible behavior due to the water content is based on the so called volumetric-isochoric decomposition of the deformation gradient Flory [1961]. The deformation gradient $\mathbf{F}$ is decoupled into dilatational and volume-preserving part as

$$\mathbf{F} = \mathrm{J}^{1/3} \bar{\mathbf{F}} \tag{1}$$

DOI: 10.1002/cnm

where $\mathrm{J} = \det(\mathbf{F})$ and $\bar{\mathbf{F}}$ is the isochoric deformation gradient.The highly non-linear behavior of the material is usually included within a finite hyperelasticity framework. It relies on the definition of a strain energy density function (SEDF). Given a SEDF in its material description $\Psi(\mathbf{C})$, and based on the dissipation inequality from classical thermodynamics (see, e.g., Truesdell and Noll [2004]) we can write, neglecting heat sources and thermal effects,

$$\Psi = \Psi_{\text{vol}}(J) + \Psi_{\text{ich}}(\bar{\mathbf{C}}). \tag{2}$$

Ψ_{vol} is related with the water content in the cardiovascular tissue. The second term $\Psi_{\text{ich}}(\bar{\mathbf{C}})$ is associated with the isochoric contribution of the deformation gradient.

The above decomposition of the SEDF naturally affects the decomposition of the stresses and the elastic tensor (see e.g. Marsden and Hughes [1994], Holzapfel [2000]). The elastic Piola-Kirchhoff stress tensor reads

$$\mathbf{S} = \mathbf{S}_{\text{vol}} + \mathbf{S}_{\text{ich}}, \tag{3}$$

where

$$\mathbf{S}_{\text{vol}} = 2\partial_{\mathbf{C}}\Psi_{\text{vol}}, \tag{4}$$

and

$$\mathbf{S}_{\text{ich}} = 2\partial_{\mathbf{C}}\Psi_{\text{ich}}(\bar{\mathbf{C}}) = 2\partial_{\bar{\mathbf{C}}}\Psi_{\text{ich}}(\bar{\mathbf{C}}) : \partial_{\mathbf{C}}\bar{\mathbf{C}} = \mathrm{J}^{-2/3}\mathbb{P} : \bar{\mathbf{S}} \tag{5}$$

where $\bar{\mathbf{S}} = \partial_{\bar{\mathbf{C}}}\Psi_{\text{ich}}(\bar{\mathbf{C}})$ is the fictitious second Piola-Kirchhoff stress and $\mathbb{P}$ is the fourth order projection tensor in the material reference defined as $\mathbb{P} = \mathbb{I} - 1/3\mathbf{C}^{-1} \otimes \mathbf{C}$.

The tangent modulus, the quantity that relates momentum fluxes and strains, is essential for a consistent finite element implementation. We can evaluate the total derivative of the $\mathbf{S}$ with respect to $\mathbf{C}$ as a direct definition, and split it again into volumetric-isochoric terms

$$\mathbb{C} = 2d_{\mathbf{C}}\mathbf{S} = 2\partial_{\mathbf{C}}\mathbf{S}_{vol} + 2\partial_{\mathbf{C}}\mathbf{S}_{ich} = \mathbb{C}_{vol} + \mathbb{C}_{ich} \tag{6}$$

The volumetric contribution to the elastic tensor becomes

$$\mathbb{C}_{\text{vol}} = 2J[p + J\partial_J p]\mathbf{C}^{-1} \otimes \mathbf{C}^{-1} - 2Jp\mathbf{C}^{-1} \odot \mathbf{C}^{-1} \tag{7}$$

The isochoric contribution is

$$\mathbb{C}_{\text{ich}} = \mathbb{P} : \overline{\mathbb{C}} : \mathbb{P}^t - 2/3\text{Tr}(J^{-2/3}\mathbf{S}_{\text{ich}})\tilde{\mathbb{P}} - 2/3[\overline{\mathbf{S}} \otimes \mathbf{C}^{-1} + \mathbf{C}^{-1} \otimes \overline{\mathbf{S}}] \tag{8}$$

where $\tilde{\mathbb{P}} = \mathbf{C}^{-1} \otimes \mathbf{C}^{-1} - 1/3\mathbf{C}^{-1} \odot \mathbf{C}^{-1}$.

Experimental results in carotid artery are extensive in the literature. However, few of them offer a complete characterization of the tissue for a specific study (same samples, species, etc). They are usually on a specific aspect of the tissue, e.g. on the mechanical properties of the wall, others on the pre-stretch state or micro-structural description of the material. And also they are from different species. Therefore it is difficult to find a complete data set and one has to rely on different studies of different samples and species.

Arterial tissue also has a characteristic structural organization. O'Connell et al. [2008] have shown that arterial fibers follow a helicoidal distribution from the outer to the inner layer. As they stated, collagen fibers are bundled around the SMC with some collagen fibrils linking the main fiber in a predominant perpendicular direction. The adventitia layer is known to have a more random distribution of collagen with almost any SMC fibroblast. In the media layer there are several sublayers, each with a preferential direction of the SMC and therefore of the collagen fibers, and elastin sheets separating these sublayers. In the case of the media layer of carotid arteries previous studies report that SMC follows an almost circumferential direction for tube-like cut samples[Garcia, 2012, O'Connell et al., 2008].

The isochocoric contribution can again be split up into different parts to model the behavior of the different components $\Psi_{\text{ich}}(\overline{I}_1, \overline{I}_4) = \Psi_{\text{iso}}(\overline{I}_1) + \Psi_{\text{ani}}(\overline{I}_4)$. Where $\overline{I}_1$ and $\overline{I}_4$ are the first and fourth invariants, respectively, of the isochoric part of the deformation. It is common to relate the behavior of the elastin with an isotropic behavior, described with a Neo-Hookean model as

DOI: 10.1002/cnm

Specimen	C_{10} [kPa]	k_1 kPa	k_2 [-]	α	ϵ
CCA media	4.31	2.19	4.15	0.13	0.05
CCA adv	0.04	7.32	66.81	0.41	0.05
ICA media	11.01	2.14	20.72	0.13	0.01
ICA adv	0.04	15.97	51.01	0.41	0.04

Table I. Material parameters for human carotid specimens in Sommer and Holzapfel [2012] fitted in Saez et al. [2014].

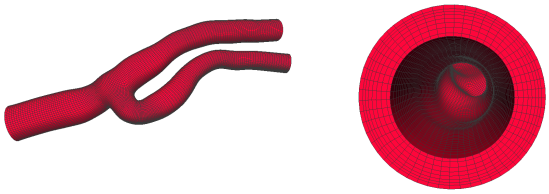

(a) Complete mesh of the CA. (b) Detail of the front side of the CA.

Figure 2. Finite element mesh of the human carotid artery.

$$\Psi_{\text{elas}}(\overline{I}_1) = \mathrm{C}_{10}[\overline{I}_1 - 3] \tag{9}$$

where C_{10} is a stress-like parameter.

Following the observations of Garcia [2012] and O'Connell et al. [2008], we can consider that the preferential direction of the fibers is almost circumferential. The collagen fibers are linked to each other by other collagen fibers, cross-linking fibrils, which we consider isotropic and perpendicular to the main fiber. We measure this density of cross-links by a factor α [Saez et al., 2014]. We can write this as

$$\begin{aligned}\Psi_{\text{ani}}(\overline{I}_1, \overline{I}_4) &= \sum_{i=1}^{N}[1-\alpha]\Psi_f^i + \alpha\left[\frac{k_1}{2k_2}[\exp(k_2[\overline{I}_1 - 3]^2) - 1] - \Psi_f^i\right] \\ &= \sum_{i=1}^{N}[1-2\alpha]\Psi_f^i + \alpha\frac{k_1}{2k_2}[\exp(k_2[\overline{I}_1 - 3]^2) - 1]\end{aligned} \tag{10}$$

where k_1 is a stress-like parameter and k_2 an adimensional material parameter. α represents the amount of cross-links, α being ≤ 0.5. $\alpha = 0$ represents no cross-links and $\alpha = 0.5$ indicates that the degree of cross-links are high enough so we can consider an isotropic distribution of the fibers. Finally,

$$\Psi_{\text{f}}(\overline{I}_4) = \frac{k_1}{2k_2}[\exp(k_2[\overline{I}_4 - 1]^2) - 1] \tag{11}$$

We consider N$= 1$ as we assume a unique family of fibers. The direction of the fibers are in the direction of maximum stress as described in Saez et al. [2014] when applying a small pressure inside the artery. For the tube-like parts, this is close to circumferential orientation. Based on experimental data of Sommer and Holzapfel [2012], Saez et al. [2014] obtained the mechanical parameters in the human carotid artery for different places, the common carotid artery (CCA) and the internal carotid artery (ICA). The results are shown in Table I.

Moreover, we use a real human geometry obtained in Alastrue et al. [2010]. We use this model to define a finite element mesh with 128,008 linear hexahedral elements (Fig. 2) which we use throughout this work. The material parameters are included linearly over the arterial length. Note that with a nonlinear constitutive equations the stresses can not be linear along the length.

DOI: 10.1002/cnm

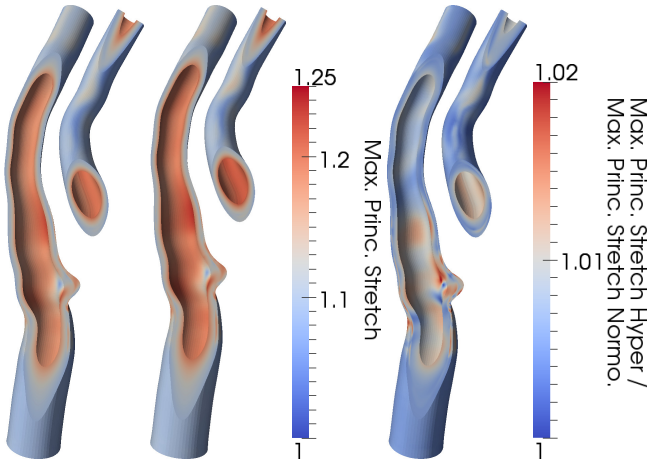

Figure 3. Maximum principal stretches at homeostatic and hypertensive pressure and ratio between stretches at hypertensive and normotensive states.

Finally, in Fig. 3 we show the maximum principal stretch at normotensive and hypertensive pressure, and the ratio between hypertensive to normotensive stretches, which we use as the trigger stimulus for the subsequent sections.

2.2. *Mass production*

In this section a synthesis and degradation of TGF-β, MMP-1 and TIMP-1 model is presented based on the description of Saez et al. [2012a]. We allow the material density to evolve in time according to the mass balance for open system thermodynamics, and adopt a source term, $\mathcal{R}$, similar to that described by Harrigan and Hamilton [1992], Kuhl and Steinmann [2003] and Saez et al. [2012a], as

$$\dot{\rho} = \mathcal{R} \qquad \text{with} \qquad \mathcal{R} = \gamma \left[\frac{\rho}{\rho^*}\right]^{-m} \lambda - \lambda^*, \tag{12}$$

where the exponent m is used for the stability of the algorithm, λ^* is the stretch of the homeostatic equilibrium state, which vary from point to point in the carotid model, and $\lambda = [\mathbf{r} \cdot \mathbf{C} \cdot \mathbf{r}]^{1/2}$ is the stretch of a fiber with orientation $\mathbf{r}$. ρ is the density of the substance at hand, ρ^* is the initial density and $\dot{\rho}$ the material time derivative of ρ.

Depending on the stretch of the SMC, which we understand to be the main driving force for these processes, the substance density will increase or decrease. In particular, we hypothesize that an increase in the stretch of the SMC will increase growth factors such as TGF-β, responsible for collagen deposition.

$$\mathcal{R}_{\text{TGF}-\beta} = \dot{\rho}_{\text{TGF}-\beta} = \gamma_{\text{TGF}-\beta} \left[\left[\frac{\rho_{\text{TGF}-\beta}}{\rho^*_{\text{TGF}-\beta}}\right]^{-m_{\text{TGF}-\beta}} \lambda_{\text{smc}} - \lambda^* \right]. \tag{13}$$

Both deposition and degradation can occur at the intracellular (collagen molecules) or extracellular (tropocollagen) levels. There have been several *in-vitro* and *in-vivo* experiments studying these processes in detail, as we discussed in the introduction. There is strong agreement that the TGF$-\beta$ plays a fundamental role in the turnover of collagen. This implies that TGF-β will be upregulated, $\mathcal{R}_{\text{TGF}-\beta} > 0$, for blood pressures above a characteristic threshold level, $\left[\rho_{\text{TGF}-\beta}/\rho^*_{\text{TGF}-\beta}\right]^{-m_{\text{TGF}-\beta}} \lambda_{\text{smc}} > \lambda^*$, downregulated, $\mathcal{R}_{\text{TGF}-\beta} < 0$, for blood pressures below $\left[\rho_{\text{TGF}-\beta}/\rho^*_{\text{TGF}-\beta}\right]^{-m_{\text{TGF}-\beta}} \lambda_{\text{smc}} < \lambda^*$, and otherwise remain constant, $\mathcal{R}_{\text{TGF}-\beta} = 0$. We further hypothesize that an increase in blood pressure will increase tissue inhibitors of metalloproteinase, TIMP, causing a decrease in metalloproteinase, responsible for collagen degradation. The mass

DOI: 10.1002/cnm

production of TIMP is also expressed as

$$\mathcal{R}_{\text{TIMP}} = \dot{\rho}_{\text{TIMP}} = \gamma_{\text{TIMP}} \left[\left[\frac{\rho_{\text{TIMP}}}{\rho^*_{\text{TIMP}}} \right]^{-m_{\text{TIMP}}} \lambda_{\text{smc}} - \lambda^* \right]. \tag{14}$$

This implies that TIMP will be upregulated, $\mathcal{R}_{\text{TIMP}} > 0$, for blood pressures above a characteristic threshold, $[\rho_{\text{TIMP}}/\rho^*_{\text{TIMP}}]^{-m_{\text{TIMP}}} \lambda_{\text{smc}} > \lambda^*$, downregulated $\mathcal{R}_{\text{TIMP}} < 0$, for blood pressures below $[\rho_{\text{TIMP}}/\rho^*_{\text{TIMP}}]^{-m_{\text{TIMP}}} \lambda_{\text{smc}} > \lambda^*$, and otherwise remain constant, $\mathcal{R}_{\text{TIMP}} = 0$. Basically, we consider the changes of TGF-β and TIMP as the primary variables, assuming that the up- and downregulation of TGF-β and TIMP is driven by the local SMC state. The material parameters $m_{\text{TGF}-\beta}, m_{\text{TIMP}} \in \mathbb{R}^+$ govern the evolution of TGF-β and TIMP respectively, while $\gamma_{\text{TGF}-\beta}, \gamma_{\text{TIMP}} \in \mathbb{R}^+$ set the sensibility of these substances to changes of the SMC stretch.

Finally, we define the source term of the MMP-1 [Saez et al., 2012a], which directly change the rate of absorption of collagen. For the sake of simplicity, we hypothesize that it directly correlates to the source term of TIMP as

$$\mathcal{R}_{\text{MMP-1}} = \gamma_{\text{MMP-1}}\, \mathcal{R}_{\text{TIMP-1}}, \tag{15}$$

where $\gamma_{\text{MMP-1}} \in \mathbb{R}^-$ defines the sensitivity of MMP-1 to changes in TIMP-1.

To solve the non-linear differential equations of collagen deposition and absorption (Eqs. 13 and 14) we adopt a standard Euler backward scheme to solve the equations implicitly in terms of the unknown ρ_0^{j+1},

$$\dot{\rho}_0 = [\,\rho_0^{j+1} - \rho_0^{j}\,]/\Delta t \tag{16}$$

for given initial conditions $\rho_0|_{t_0=0} = \rho_0^*$. The temporal discretization is given by dividing the time interval $\mathcal{T}$ into s discrete subintervals, $\mathcal{T} = \bigcup_{j=0}^{s-1}[t^j, t^{j+1}]$, with a time increment $\Delta t = t^{j+1} - t^j \geq 0$. We linearize the evolution equations, Eq. 13 and 14, for TGF-β and TIMP to obtain their residual forms to be embedded in a Newton-Raphson iterative scheme. We refer to Saez et al. [2013] for the complete development of these equations.

2.2.1. Material fitting in hypertension-induced collagen deposition and absorption Collagen turnover in disease conditions can be attributed to changes in the deposition and absorption of MMP-1 and TGF-β. We use the data given in Laviades et al. [1998], who investigated alterations in collagen type I, matrix metalloproteinase, and inhibitors of matrix metalloproteinase to fit our material parameters. These authors reported an increase of 178.9%, from 641±31 ng/mL to 1147±55, in total TIMP-1 and a decrease in total MMP-1 density of 18.07%, from 56±2 ng/mL to 47±1 ng/mL. TGF-β and collagen has also been reported to be upregulated in hypertensive patients. We take as baseline values of TGF-β a concentration of 35ng/mL [Schaan et al., 2007], and the 4.2-fold increase in hypertensive patients reported by [Porreca et al., 1997]. The material parameters obtained are presented in Table II.

Table II. Collagen turnover model. Material parameters for hypertensive case study.

material parameter	value	units
$\rho^*_{\text{TGF}-\beta}$	0.035	[μg/mL]
$\rho^*_{\text{TIMP-1}}$	0.459	[μg/mL]
$\rho^*_{\text{MMP-2}}$	0.0353	[μg/mL]
$m_{\text{TGF}-\beta}$	0.007	[$-$]
$m_{\text{TIMP-1}}$	0.016	[$-$]
$\gamma_{\text{TGF}-\beta}$	40	[ms/mm^2]
$\gamma_{\text{TIMP-1}}$	80	[ms/mm^2]
$\gamma_{\text{MMP-1}}$	- 80	[ms/mm^2]

Fig. 4 shows the evolution of the TGF-β, TIMP-1 and MMP-1 content, respectively, in response to hypertension conditions.

DOI: 10.1002/cnm

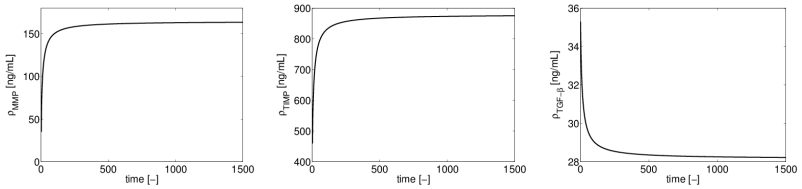

(a) Evolution of TGF-β (b) Evolution of TIMP-1 (c) Evolution of MMP-1

Figure 4. Evolution of TGF-β, TIMP-1, and MMP-1 concentrations involved in progressive collagen turnover.

2.3. Diffusion through the vessel wall

In this section we deal with the mass transport problem of the substances described above. The substances secreted in the media layer are transport trough out the adventitia. The mass transport is governed by diffusion and convection phenomena.

Considering changes in mass (see e.g. the monographs by Welty et al. [2008], Deen [2011]), the mass balance have to fulfill that the flux of mass and the mass source be in equilibrium with the change of material density. Although the geometry of the elastin sheet could modify the transport results we will neglect it in this work. Also the diffusion and permeability parameters could be anisotropic but for simplicity and given the steady-state considered we have opted for an isotropic definition. The partial differential equation is managed numerically to be solved within a Finite Element scheme in the commercial software ABAQUS with standard elements and formulation. By evaluating in the domain Ω_0 and applying Divergence Theorem we obtain

$$\int_{\Omega} \mathrm{D}_t \rho \mathrm{dV} = \int_{\delta\Omega} \mathbf{J} \cdot \mathbf{n} \mathrm{dV} + \int_{\Omega} \mathcal{R} \mathrm{dV}, \tag{17}$$

where ρ is the material density, $\mathbf{J}$ the mass flux and $\mathcal{R}$ the source of mass. The domain of interest, as previously stated will be denoted by Ω.

The boundary of the problem (Eq. 18) $\delta\Omega$ is conditioned by Neumann boundary conditions over $\delta\Omega$. In particular, we consider the following set of boundary conditions:

$$\begin{gathered} \mathbf{J} \cdot \mathbf{n} = 0 \ \text{ on } \ \delta\Omega_{endo} \\ \mathbf{J}^{layer+} \cdot \mathbf{n}^{layer+} = \mathbf{J}^{layer-} \cdot \mathbf{n}^{layer-} \ \text{ on } \ \delta\Omega_{layer} \\ \mathbf{J}^{ext} \cdot \mathbf{n}^{ext} = 0 \ \text{ on } \ \delta\Omega_{ext} \end{gathered} \tag{18}$$

where *endo*, *layer* and *ext* represent the endothelium, the media-adventitia interface layer and the external face of the adventitia, respectively.

As demonstrated in the previous section, the mass transport in arterial tissue is a diffusion-convection problem that we solve here for the steady state.

To recover these phenomena the flux term is given by

$$\mathbf{J} = -\mathrm{D}_{eff} \nabla \rho_0 + \rho_0 \mathrm{D}_t \mathbf{u} \tag{19}$$

where the first term represents the diffusive contribution and is driven by density gradients. The second term represents the convective contribution and it is assumed to be controlled by pressure gradients with $\mathbf{u}$ being the displacement vector of the fluid. Note that this displacement is only due to the pressure gradient and is not a function of the movement of the solid.

Diffusion coefficients are related to the molecular size and the size of the porous media which the molecule passes through. For the three substances considered in this work, is given by the Stokes-Einstein Equation [Einstein, 1905] as

$$D_{\infty}[m^2/s] = \frac{k_B T}{6\pi\mu a}, \tag{20}$$

DOI: 10.1002/cnm

where $k_B = 1.38 \cdot 10^{-23}[J/K]$ is the Boltzmann constant, T = 293[K] is the absolute temperature which remains constant, $\mu = 4 \cdot 10^{-3}[N.s/m2]$ is the viscosity of the fluid and a is the particle radius obtained by superposing a sphere that contains the particle.

Diffusivity in a fiber-matrix media was derived by Ogston et al. [1973] and subsequently used by Kim and Tarbell [1994] among others. The effective diffusion coefficient can be expressed as

$$D_m[m^2/s] = D_\infty exp\left[-[(1-\epsilon)^{0.5}(1+a/r_f)]\right], \tag{21}$$

where r_f is the collagen fiber radius which has an average value of $1\mu m$ (Huang and Tarbell [1997], Yang [2008]), $\epsilon = 1 - V_f$ is the void fraction and V_f is the fiber volume fraction which, based on data given by Huang and Tarbell [1997] and O'Connell et al. [2008], is approximately equal to 45%. Moreover, the contribution of the presence of SMC can be recovered [Huang and Tarbell, 1997] by

$$D_{eff}[m^2/s] = \frac{1}{1-\epsilon_{SMC}} \frac{1}{f(\epsilon_{SMC})} D_m, \tag{22}$$

where $f(\epsilon_{SMC}) = 2.3899$ given a SMC volume fraction of $\epsilon_{SMC} = 25\%$ [Huang and Tarbell, 1997].

Table III. Collagen turnover model. Material parameters for hypertensive case study.

	TGF-β	TIMP-1	MMP-1
$D_\infty[m^2/s] \cdot 10^{-12}$	1.9227	3.8455	2.1974
$D_m[m^2/s] \cdot 10^{-13}$	8.081	16.13	9.229
$D_{eff}[m^2/s] \cdot 10^{-13}$	4.444	8.887	5.075

In order to discern if the diffusion and convective phenomena are important in mass transport within the arterial wall it is usual to calculate the Pèclet number (Pe) (Eq. 23). For Pe $>> 1$ convection has to be studied while for Pe $<< 1$ diffusion dominates the problem. The Pèclet number for the present problem is

$$\text{Pe} = \frac{\text{vl}}{\text{D}_{eff}} \approx 10^2 \tag{23}$$

where the fluid velocity v takes a mean value of 0.05 $[\mu m/s]$ [Levick, 1987, Wang and Tarbell, 1995], the thickness l =1-0.6 [mm] and the effective diffusive parameters given in Eq. 22, gives a Pèclet number in the order of hundreds. A Pèclet number higher than 1 shows necessity of taking into account the convective phenomena.

Therefore, we include the convective term into the model. We can obtain the velocity through the solid by means of Darcy's law (Eq. 24). Note therefore, that Navier-Stokes equations are not used and velocity is not obtained independently but based on pressure gradients.

$$\nabla \text{p} = -\mu/K_p \text{D}_t \mathbf{u} \tag{24}$$

where p is the pressure and μ the viscosity of the fluid. Note, therefore, that the fluid movement is only due to the pressure gradient. Also due to the quasi-static treatment of the solid part this is a reasonable assumption. Some authors [Tada and Tarbell, 2002] have also used the Brinkman equation [Brinkman, 1947] to model the transmural flow.

The parameter required in order to study the convection related term in blood vessels, according to the fiber-matrix theory, is the hydraulic permeability K_p which can be calculated with the Kozeny-Carman equation as discussed by Curry [1984].

$$K_p[m] = \frac{r_f^2 \epsilon^2}{4c_k(1-\epsilon)^2} = 1.389e-13, \tag{25}$$

Prepared using cnmauth.cls
DOI: 10.1002/cnm

where c_k is the Kozeny constant with a value equal to 5 [Huang and Tarbell, 1997]. Again the permeability has to be recalculated to take into account the SCM distribution. Similarly,

$$K_{p_{eff}}[m] = K_p \frac{1 - \epsilon_{SMC} - 0.3058\epsilon_{SMC}}{1 - \epsilon_{SMC} + 0.3058\epsilon_{SMC}} = 7.9721e - 14 \tag{26}$$

2.4. Collagen remodeling

In our particular case, we have considered that substances are transported by diffusion and convection phenomena. Although a fully implicit formulation is also feasible, this involves a much more complicated computational model. We refer to Kuhl [2003] where a complete definition of open systems and its numerical implementation is addressed. The mass source, based on the work of Saez et al. [2012a], is defined as

$$\hat{\mathcal{R}}_{\text{col}} = \gamma_{\text{dep}} \hat{\mathcal{R}}_{\text{TGF}-\beta} + \gamma_{\text{abs}} \hat{\mathcal{R}}_{\text{MMP-1}}. \tag{27}$$

$\hat{\mathcal{R}}_{\text{TGF}-\beta}$ and $\hat{\mathcal{R}}_{\text{MMP-1}}$ are actual amount of TGF-β and MMP-1 at every integration point after the mass transport phenomena. $\gamma_{\text{dep}}, \gamma_{\text{abs}} \in \mathbb{R}^+$ denote the sensitivities of collagen deposition and absorption in response to changes in TGF-β and MMP-1, respectively. The material parameters are summarized in Table IV.

Given this evolution equation for the collagen turnover, three different scenarios can be considered: an increase in mass $\hat{\mathcal{R}}_{\text{col}} > 0$, a decrease $\hat{\mathcal{R}}_{\text{col}} < 0$, or maintenance of the collagen content, $\hat{\mathcal{R}}_{\text{col}} = 0$. These scenarios have to be constrained by the following inequalities in order to ensure the correct collagen turnover.

$$\hat{\mathcal{R}}_{col} \begin{cases} > 0 & \text{if} \quad \lambda_{\text{smc}} > \lambda^* \mapsto \gamma_{\text{dep}}/\gamma_{\text{abs}} > \hat{\mathcal{R}}_{\text{MMP-1}}/\hat{\mathcal{R}}_{\text{TGF}-\beta} \\ < 0 & \text{if} \quad \lambda_{\text{smc}} < \lambda^* \mapsto \gamma_{\text{dep}}/\gamma_{\text{abs}} < \hat{\mathcal{R}}_{\text{MMP-1}}/\hat{\mathcal{R}}_{\text{TGF}-\beta} \\ = 0 & \text{if} \quad \lambda_{\text{smc}} = \lambda^* \mapsto \gamma_{\text{dep}}/\gamma_{\text{abs}} = \hat{\mathcal{R}}_{\text{MMP-1}}/\hat{\mathcal{R}}_{\text{TGF}-\beta} \end{cases} \tag{28}$$

material parameter	value	units
ρ^*_{col}	1	[g/mL]
γ_{dep}	90000	[–]
γ_{abs}	400000	[–]

Table IV. Material parameters of the collagen turnover model for the hypertensive case study [Saez et al., 2012a].

For the sake of simplicity, we consider an explicit algorithm. We rewrite the update of the collagen mass as

$$\rho^{j+1}_{\text{col}} \quad = \quad \rho^{j}_{\text{col}} \quad + \quad \hat{\mathcal{R}}_{\text{col}} \quad \Delta t = 0 \tag{29}$$

where the residual is no longer required.

In addition, we take into account the results given by Diez et al. [1995], where the serum concentration of procollagen peptides was examined. The authors studied the concentration of procollagen type I carboxy terminal peptide (PIP), which has been proposed as a marker of synthesis of the collagen type I, displaying an increase of 28%. The same authors found that the carboxy-terminal telopeptide of collagen type I (CITP), a marker of extracellular collagen degradation, was increased by approximately 9% [Laviades et al., 1998]. These data are used in the model to evaluate the increase or decrease in the collagen content.

Due to the collagen turnover the arterial wall change its mechanical properties. Recalling the baseline SEDF described in Eq. 10, we will modify the collagen SEDF to reflect its turnover as $[\rho_{col}/\rho^*_{col}]\Psi_{col}$.

We can now obtain the stress tensor and its linearization with respect to deformations for the FE implementation. The Piola-Kirchoff stress tensor reads

DOI: 10.1002/cnm

$$\mathbf{S}_{col} = [\rho_{col}/\rho^*_{col}] \quad \partial_{\mathbf{C}}\Psi_{col}. \tag{30}$$

Given that we do not apply a fully implicit formulation since we neglect dependencies of the mass sources with respect to the strain, the tangent operator is reduced to

$$\mathbb{C}_{col} = \partial_{\mathbf{C}}\mathbf{S}_{col}\big|_{\mathbf{C}}. \tag{31}$$

3. RESULTS

3.1. Mass source

In this section we present the results of the mass production in the real carotid artery based on the model and material parameters presented above. The results are shown in a longitudinal cut. In Fig. 5 we show the evolution of the of TGF-β, TIMP-1 and MMP-1 production, respectively, in the media layer for different times. The results correlate well with the range of values presented in the experimental findings reported in Section 2.2.1. The distributions of the mass production of each substance match with the increases in the stretches field shown in the previous section. Mass production is higher at the beginning of the carotid bifurcation while the section of the CCA before the bifurcation presents lower rates of production. The rest of the carotid shows very similar production rate values due to the uniform stretch field.

In Fig. 6 we present the evolution of each substances at six points of interest in the carotid artery. The substances also follow a saturation-like behavior similar to that shown in the analytic results of the previous section. The values of these points, as in the whole artery, stay in the range of values shown in the previous section. The mass production in the carotid artery show an inhomogeneous mass production of each substance varying with location.

DOI: 10.1002/cnm

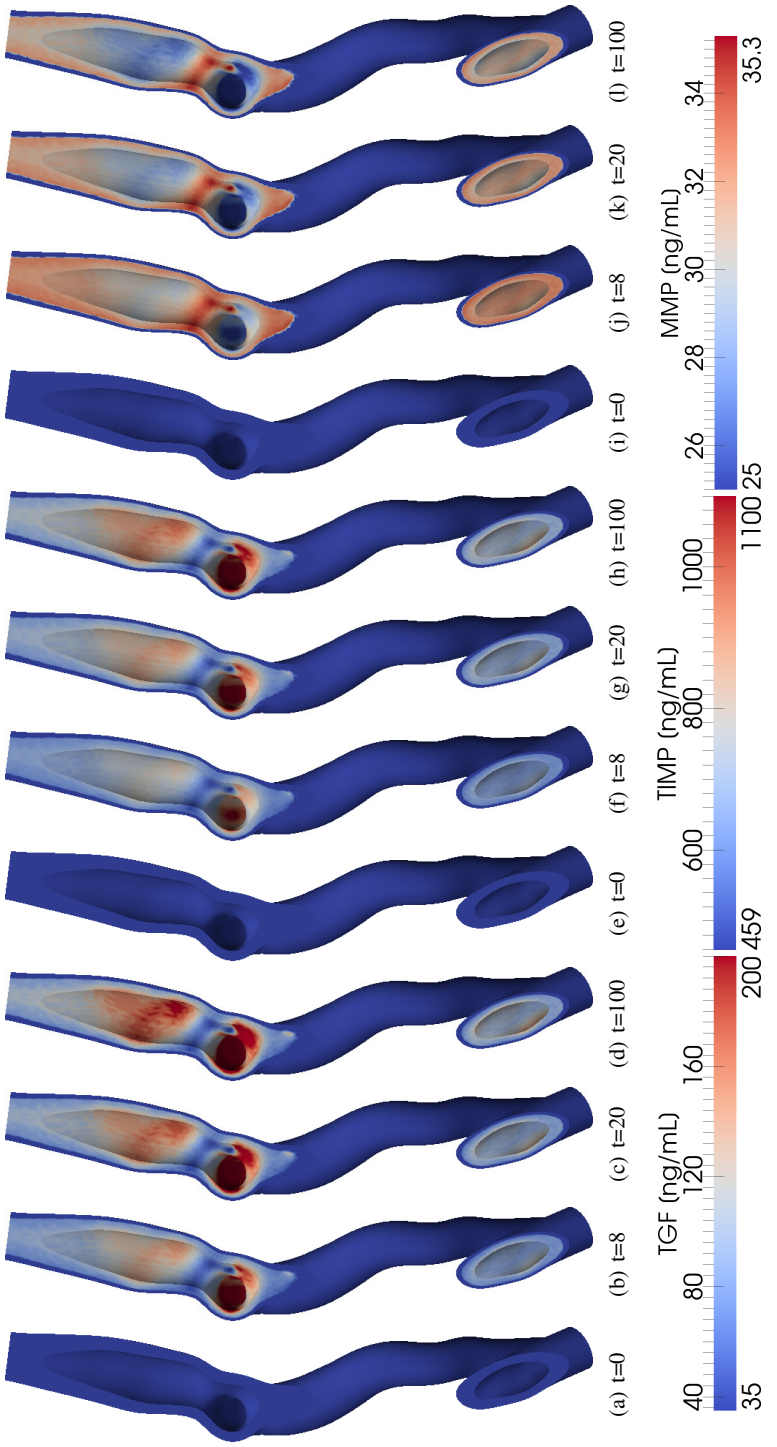

Figure 5. Evolution of the mass production of TGF-β, TIMP-1 and MMP-1 due to SMC activity in different transversal cuts.

DOI: 10.1002/cnm

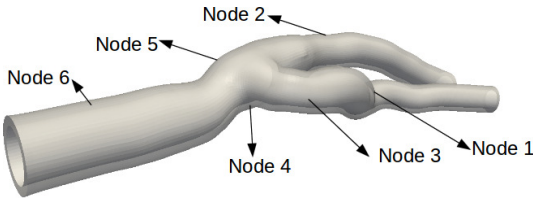

(a) Featured points in the media layer.

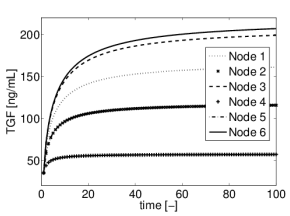

(b) Evolution of TGF-β.

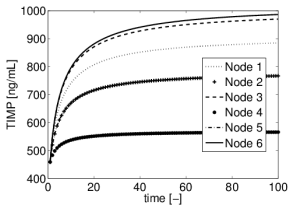

(c) Evolution of TIMP-1

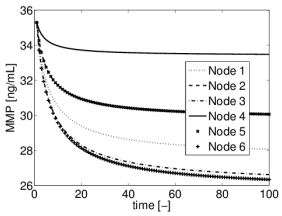

(d) Evolution MMP-1

Figure 6. Evolution of the mass production of (a) TGF, (b) TIMP-1 and (c) MMP-1 at six featured point due to SMC activity.

3.2. Mass transport

In this section we present the results of the mass transport from the media layer through the arterial wall. The results are presented in a longitudinal cut and only for the adventitia layer, for the sake of clarity. Note that fibroblast are located mainly in the adventitia layer and are the main responsibles for the synthesis of collagen molecules. In Figs. 7 we show the evolution of the TGF-β, TIMP-1 and MMP-1 in the adventitia layer for different times. The qualitative results show that substances in the adventitia layer maintain a similar concentration, although slightly below the concentration in the media layer where these substances are synthesized. A higher mass transfer rate appears for the TIMP given its higher diffusion coefficient. We also show in Fig. 8 the mass evolution of the three substances at the six featured points highlighted in the figure.

DOI: 10.1002/cnm

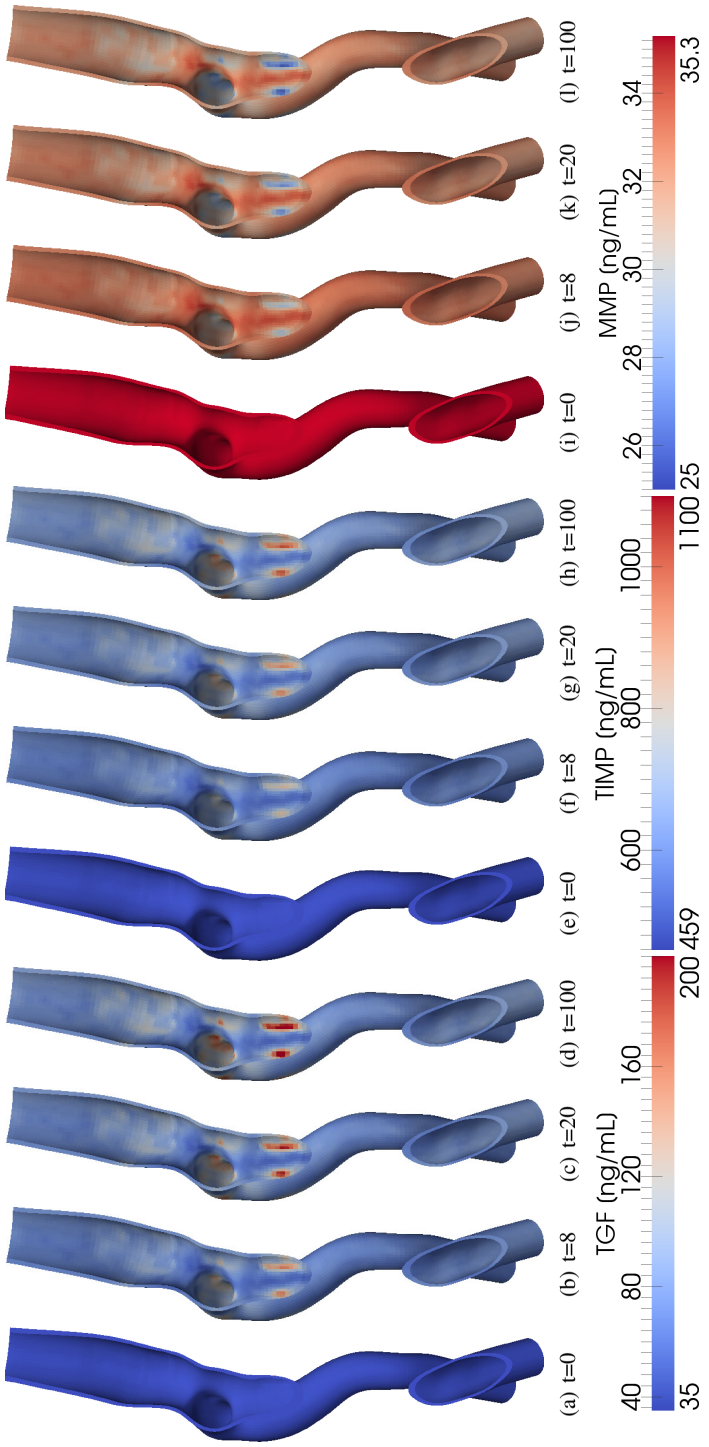

Figure 7. Evolution of the TGF-β, TIMP-1 and MMP-1 content in the adventitia layer due to mass transport in the carotid wall in different transversal cuts.

DOI: 10.1002/cnm

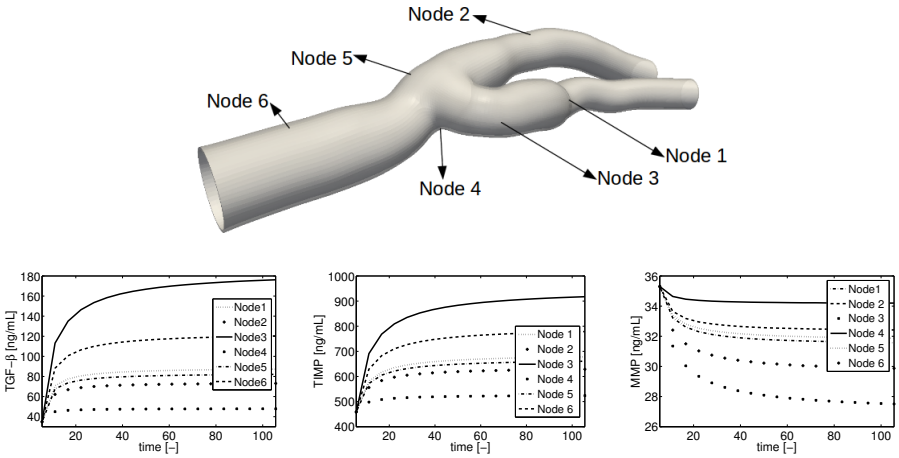

(b) Evolution of TGF$-\beta$. (c) Evolution of TIMP-1. (d) Evolution of MMP-1.

Figure 8. Evolution of the mass transport in the adventitia of TGF (a), TIMP-1 (b) and MMP-1 (c) at six featured points due to SMC activity.

3.3. Collagen turnover

In this last section we present the results corresponding to the increment of collagen content. The results are presented in 4 different longitudinal cuts in Fig. 9 and in Fig. 10 for the media and adventitia layer, respectively. The results show the evolution of the collagen turnover due to the balance of TGF-β and MMP-1. The increase in collagen content is higher in the media than in the adventitia layer. Note that the concentrations of TGF-β and MMP-1 are lower in the adventitia after the transport of these substances from the media layer, where they are synthesized. The evolution in the media layer ranges from an average value of 8-10$\%$ to a maximum of 45-50$\%$, with some peaks of 80$\%$.

Following the TGF-β, MMP-1 and TIMP-1 evolution in Fig. 8, collagen turnover in the six nodes of interest shows averaged increases of collagen in the media layer with maximum of $\approx 35\%$, mean increases of $\approx 15\%$ and minimum at 3%. Results in the featured points in the adventitia layer shows mean values of $\approx 10\%$, with maximum at 30% and minimum around $3-5\%$.

Given the Neumann boundary conditions, increases in the collagen content lead to a contraction in the lumen radius while maintaining similar stress levels over the arterial wall. This means that the consequence of the collagen turnover is the diminishing of the lumen radius but without an increase in the stresses in the arterial wall. The contraction values of the carotid lumen due to the increase in the collagen content are shown in Table V for different slices of interest. Several slices of the carotid are investigated where the contraction level (diameters radius before and after collagen turnover) varies from $\approx 10-20\%$.

4. DISCUSSION

Arterial tissue undergoes important changes in its mechanical properties during its lifetime [Jani and Rajkumar, 2006] but also because of different pathologies. In this work we have focused on the modeling of collagen turnover that occurs in hypertensive patients [Bishop et al., 1994, Laviades et al., 1998, McNulty et al., 2006]. The main consequence of the increase in collagen content is the stiffening of the arterial wall.

To this end we have developed a *computational framework* to study the collagen turnover in hypertensive diseases. We first computed a two-step simulation of a carotid artery in normotensive and hypertensive conditions. The tissue, and therefore the SMC, undergoes an over-stretching due to the high pressure of hypertension conditions. We consider this increase in the SMC stretch as

Prepared using cnmauth.cls
DOI: 10.1002/cnm

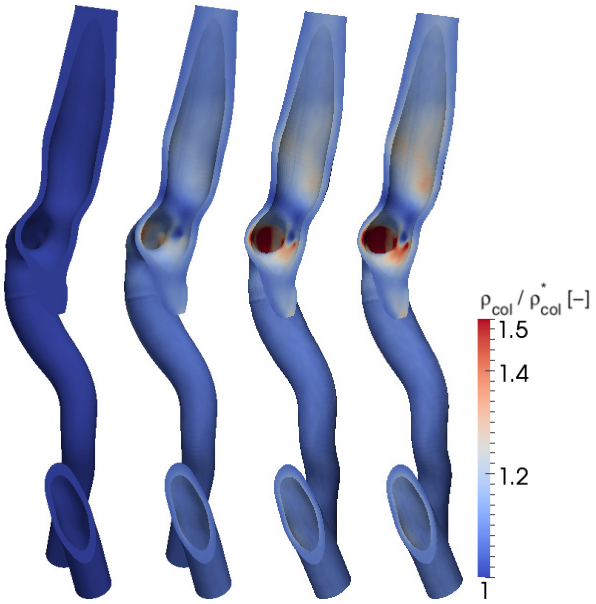

Figure 9. Evolution of the collagen content in ρ_{col}/ρ^*_{col} due to fibroblast release and MMP-1 degradation on the media layer.

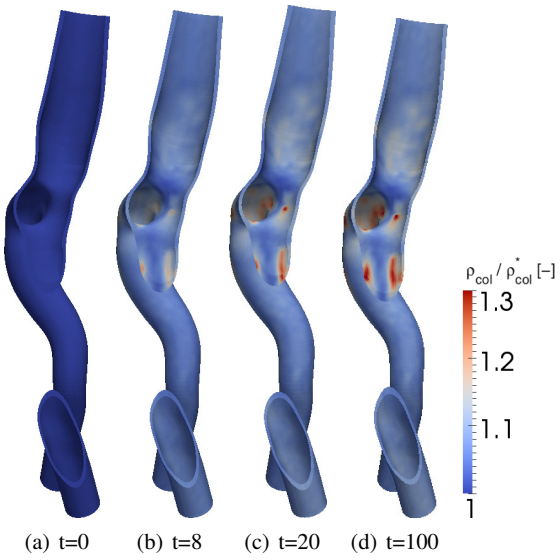

Figure 10. Evolution of the collagen content in ρ_{col}/ρ^*_{col} due to fibroblast release and MMP-1 degradation on the adventitia layer .

the trigger that boosts the synthesis of different substances. At this point we computed the amount of paracrine and autocrine TGF-β and TIMP-1 secreted by the SMC and the subsequent imbalance of MMP-1, that we believe, as described by references in the introduction section, are the most important processes to take into account. We used mean difference stretches to fit the experimental data of these substances. In the next step we simulated the mass transport of these substances from the media layer through the adventitia layer. The interaction of MMP-1 with collagen as well as the stimulation of fibroblast by TGF-β causes the collagen content to change. We compute the substances turnover of a patient specific carotid geometry in a finite element model.

Prepared using cnmauth.cls
DOI: 10.1002/cnm

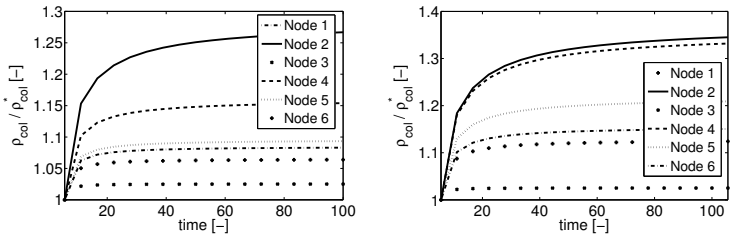

(a) Collagen evolution in adventitia layer. (b) Collagen evolution in media layer.

Figure 11. Evolution of the collagen content in the media and adventitia stress at the six nodes depicted in Fig. 8.

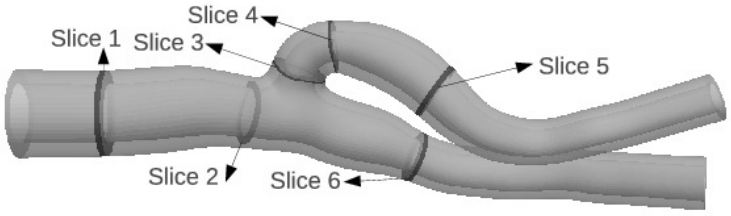

	Slice 1	Slice 2	Slice 3	Slice 4	Slice 5	Slice 6
Initial radius [mm]	4.8177	3.8292	2.9090	2.6611	3.5053	3.1023
Final radius [mm]	4.0444	3.2109	2.6538	2.1879	2.8946	2.6078
Contraction [%]	19.21	19.25	9.61	21.62	11.98	18.89

Table V. Variation in the lumen diameters at different positions due to the increase in collagen content.

The turnover of the different constituents in the arterial wall has been studied by mathematical and numerical models. Most of these models have been based on purely mechanical stimuli [Kuhl et al., 2003] leaving out a substantial number of biochemical processes. There are some models that deal with the turnover of the arterial constituents very successfully but they tend to be analytical, for example in the context of mixture theory [Alford and Taber, 2008, Humphrey and Rajagopal, 2003], and use very simple geometries [Alford et al., 2008, Figueroa et al., 2009]. These mixtures models for turnover are local and do not consider mass transport phenomena. Moreover they are based only on mechanical variables and they not take into account the real biological substances. Here we have modeled and computed for the first time, as far as our knowledge go, the first simulation in a finite element framework based on the real biological substances that lead to the remodeling process in the arterial tissue.

Our results on the *substances turnover* (TGF-β, TIMP and MMP-1) correlate with experimental results reported in Laviades et al. [1998], Schaan et al. [2007] and Porreca et al. [1997] as we demonstrated in Section 2.2.1. We discussed here about the MMPs-TIMPs relation. In terms of the *collagen content*, our model shows increases of $\approx 15\%$ in the media layer and of $\approx 10\%$ in the adventitia. Maxima were at 35% and 25% in the media and adventitia layer respectively. These results are comparable with the experimental findings in, e.g., Bagshaw et al. [1987] reporting a 37% increase in collagen content and Hu et al. [2007b] reporting a 30% increase. Hu et al. [2008] also report increases of 15% in hypertension following a decrease to normal values. They hypothesized that this was due to the enhanced collagen degradation by MMPs. Eberth et al. [2010] also observed that the collagen content rise up to $\approx 20\%$ in an extensive model of carotid remodeling in altered pulsatility. Collagen turnover has a direct consequence on arterial compliance and distensibility due to the stiffening that the collagen produces. Our results reflect this behavior in terms of a loss of distensibility. This stiffening has been reported by, e.g., Hayashi et al. [1980], Hajdu and Baumbach

DOI: 10.1002/cnm

[1994], Hu et al. [2007b,a] and Eberth et al. [2011]. All these works show the stiffening that our model predicts. Note, also, that we have studied the effect of density changes in collagen but not if the orientation of these fibers does. As far as our knowledge goes, collagen density changes but not its distribution.

Our model predict a contraction of the lumen. There are data in literature showing a decrease or increase of the lumen diameter. Wiener et al. [1977] reported a decrease of the lumen dialeter of 9%. Schofield et al. [2002] also reported a reduction of 15.7% in the lumen diameter in small human arteries. Boutouyrie et al. [1999] and Eberth et al. [2010], however, showed an increase of 7.8% and 11.1% of the internal diameter respectively. In this regard, as we mentioned before, data in literature shown many different results. The previous mentioned works on the effects of hypertension include more effects as the thickening of the arterial wall (see, e.g., Owens et al. [1981]) or the dysfunctional endothelial NO which can dilate or contract the artery. We are not considering these aspects all together but looking individually at the effect of collagen remodeling due to hypertensive disease. Since we only focused on the stiffening of the arterial tissue, we can not conclude that our model could, up to day, predict accurately this diameter variation since other effects as the thickening or NO vasodilating could influence the results. Future work will be focused on include the effects of myogenic tone, NO and our previous model on arterial thickening [Saez et al., 2014], all together, to give a clue about this geometrical effect.

There are some *limitations* in the present approach. First, we have left out of this study a very important aspect of SMC, the myogenic tone, which is the trigger element of our model as already discussed in the introduction section. SMC produces the so called myogenic tone which activates the contraction of the cell and makes arteries adapt the lumen to maintain the same mechanical state in the wall. There are other biological aspects accurring during hypertension that we left out of our model, but as we stated, we believe the ones considered here are the most relevants ones. Also, we looked to the beginning of the precess where all the quantities are unbalanced. However, these substances, as e.g. TGF-β, turn to normal values. We are, however, not considering the long term scenario. We took out of our model residual stresses which can modify the stress distribution across the different layers Delfino et al. [1997]. Although absolute value of stretches could change when residual stresses are included the difference between the normotensive and hypertensive conditions would not vary remarkably. Residual stresses in the arterial tissue when bifurcation is not completely well defined theoretically and we wanted to keep the model as simple as possible to investigate the individual effect of the unbalanced substances and collagen turnover.

In terms of computational issues, the model could also be carried out in a more compact scheme. We did our simulations in a sequential way. However, given the differences in the time scales of each process, mass transfer, transport and collagen turnover, the splitting into separate processes is a reasonable approach. Another issue in the computational treatment of the problem is that the time-related parameters do not have a clear physical meaning. Finally, the number of material parameters is also a drawback although this is a common issue in almost any computational model on literature.

Better experimental data in controlled environment of the autocrine and paracrine function by SMC and fibroblast for different mechanical stimuli are also required. The subsequent collagen turnover should also be better characterized. Experimental tests with singles cell or a controlled population, where the substances released and collagen turnover could be measured, would allow to a better fitting of our model parameters. This procedure would also allow to reproduce more general cases and give new insights in unknown issues by experimentalist. However, as far as we know, this is not available. Although these values can be measured easily in a controlled test it is not that easy in-vivo. Collagen turnover occurs at different degrees and depending on which point of the carotid we are looking at. More accurate values of the collagen content through the different layers and position would be helpful data that have neither been measured previously. Our results can predict the differences on collagen content at different spots that experiments could provide.

Besides overcoming the limitations mentioned in the last paragraph, the model will, if the previous limitations could be overcame, be easily extrapolated to simulate collagen turnover in other cardiovascular tissue presented in the heart [Diez and Laviades, 1997], aorta [Wolinsky, 1971], and other cardiovascular pathologies such as aneurysms. Our approach, more focused on the actual

DOI: 10.1002/cnm

biological background that other previous models can help to clinicians and biologist to advance in treatment protocols. Planning patient-specific treatments is a very costly procedure. Computational models are in the way of helping experimentalist to understand and control better these puzzling problems.

As **conclusion**, in this work we have developed a mechano-chemical model of the process of collagen turnover in the vessel wall during hypertension. As far as our knowledge goes, we have modeled for the first time the mechanobiology of the collagen turnover in cardiovascular tissue. We have included different substances secreted by SMC and fibroblast that at the end make the collagen density to vary. We have include this in a general finite element framework. Given experimental data from literature of these biological substances we have been able to reproduce the final increase of collagen density and the following stiffening.

5. ACKNOWLEDGEMENT

Pablo Saez acknowledge support from the Spanish Ministry of Research and Innovation through the grant BES-009-028593. Financial support for this research was provided by the Spanish Ministry of Science and Technology through research project DPI2013-44391-P, the Instituto de Salud Carlos III (ISCIII) through the CIBER initiative. CIBER-BBN is an initiative funded by the VI National R&D&i Plan 2008-2011, Iniciativa Ingenio 2010, Consolider Program, CIBER Actions and financed by the Instituto de Salud Carlos III with assistance from the European Regional Development Fund.

REFERENCES

V. Alastrue, A. Garcia, E. Pena, J. F. Rodriguez, M. A. Martinez, and M. Doblare. Numerical framework for patient-specific computational modelling of vascular tissue. *Int J Numer Method Biomed Eng*, 26(1):35–51, January 2010.

P. W. Alford and L. A. Taber. Computational study of growth and remodelling in the aortic arch. *Computer Methods In Biomechanics and Biomedical Engineering*, 11(5):525–538, 2008.

Patrick Alford, Jay Humphrey, and Larry Taber. Growth and remodeling in a thick-walled artery model: effects of spatial variations in wall constituents. *Biomech Model Mechan*, 7:245–262, 2008.

R. J. Bagshaw, S. J. Barrer, and R. H. Cox. Connective-tissue analysis of the canine circle of willis in hypertension. *Neurosurgery*, 21(5):655–659, November 1987.

J. E. Bishop and G. Lindahl. Regulation of cardiovascular collagen synthesis by mechanical load. *Cardiovasc Res*, 42(1):27–44, April 1999.

J. E. Bishop, S. Rhodes, G. J. Laurent, R. B. Low, and W. S. Stirewalt. Increased collagen-synthesis and decreased collagen degradation in right-ventricular hypertrophy induced by pressure-overload. *Cardiovas Res*, 28(10):1581–1585, October 1994.

J. E. Bishop, R. Butt, K. Dawes, and G. Laurent. Mechanical load enhances the stimulatory effect of pdgf on pulmonary artery fibroblast procollagen synthesis. *Chest*, 114(1):25S–25S, July 1998.

R.A. Boerboom, N. J. Driessen, J.B. Niels, C.V. Bouten, V.C. Carlijn, J.M. Huyghe, F. P. Baaijens. Finite Element Model of Mechanically Induced Collagen Fiber Synthesis and Degradation in the Aortic Valve. *Ann Biomed Eng* 31, 1040–1053.

W. A. Border and N. A. Noble. Transforming growth-factor-beta in tissue fibrosis. *New Engl J Med*, 331(19):1286–1292, November 1994.

DOI: 10.1002/cnm

P. Boutouyrie, C. Bussy, P. Lacolley, X. Girerd, B. Laloux, and S. Laurent. Association between local pulse pressure, mean blood pressure, and large-artery remodeling. *Circulation*, 100(13): 1387–1393, September 1999.

H. C. Brinkman. A calculation of the viscous force exerted by a flowing fluid on a dense swarm of particles. *Appl Scientific Res*, 1(1):27–34, 1947.

H. Brunner, J. R. Cockcroft, J. Deanfield, A. Donald, E. Ferrannini, J. Halcox, W. Kiowski, T. F. Luscher, G. Mancia, A. Natali, J. J. Oliver, A. C. Pessina, D. Rizzoni, G. P. Rossi, A. Salvetti, L. E. Spieker, S. Taddei, and D. J. Webb. Endothelial function and dysfunction. part ii: Association with cardiovascular risk factors and diseases. a statement by the working group on endothelins and endothelial factors of the european society of hypertension. *Journal of Hypertension*, 23(2): 233–246, February 2005.

J. M. Burke and R. Ross. Synthesis of connective tissue macromolecules by smooth muscle. *International review of connective tissue research*, 8:119–57, 1979.

R. P. Butt and J. E. Bishop. Mechanical load enhances the stimulatory effect of serum growth factors on cardiac fibroblast procollagen synthesis. *J Mol Cell Cardiol*, 29(4):1141–1151, April 1997.

R. P. Butt, G. J. Laurent, and J. E. Bishop. Collagen production and replication by cardiac fibroblasts is enhanced in response to diverse classes of growth-factors. *Eur J Cell Biol*, 68(3):330–335, November 1995.

L. M. Cancel, A. Fitting, and J. M. Tarbell. In vitro study of ldl transport under pressurized (convective) conditions. *Am J Physiol-Heart C*, 293(1):H126–H132, July 2007.

P. Chamiot Clerc, J. F. Renaud, J. Blacher, M. Legrand, J. L. Samuel, B. I. Levy, J. Sassard, and M. E. Safar. Collagen i and iii and mechanical properties of conduit arteries in rats with genetic hypertension. *Journal of vascular research*, 36(2):139–46, 1999.

P. A. Curmi, L. Juan, and A. Tedgui. Effect of transmural pressure on low-density-lipoprotein and albumin transport and distribution across the intact arterial-wall. *Circ Res*, 66(6):1692–1702, June 1990.

R. M. Curry. Mechanics and thermodynamics of transcapillary exchange. In *The Cardiovascular System. Microcirculation*. American Physiological Society, 1984.

Mahsa Dabagh, Payman Jalali, YrjoT. Konttinen, and Pertti Sarkomaa. Distribution of shear stress over smooth muscle cells in deformable arterial wall. *Medical & Biological Engineering & Computing*, 46(7):649–657, 2008.

Mahsa Dabagh, Payman Jalali, and Yrjo T. Konttinen. The study of wall deformation and flow distribution with transmural pressure by three-dimensional model of thoracic aorta wall. *Medical Engineering & Physics*, 31(7):816 – 824, 2009a.

Mahsa Dabagh, Payman Jalali, Pertti Sarkomaa, and Yrjo Konttinen. Molecular transport through arterial wall composed of smooth muscle cells and a homogeneous fiber matrix. *Journal of Porous Media*, 12(3):201–212, 2009b.

W. M. Deen. *Analysis of Transport Phenomena*. Oxford University Press, 2011.

A. Delfino, N. Stergiopulos, J. E. Moore, and J. J. Meister. Residual strain effects on the stress field in a thick wall finite element model of the human carotid bifurcation. *J Biomech*, 30(8):777–786, August 1997.

J. Diez and C. Laviades. Monitoring fibrillar collagen turnover in hypertensive heart disease. *Cardiovas Res*, 35(2):202–205, August 1997.

DOI: 10.1002/cnm

J. Diez, C. Laviades, G. Mayor, M. J. Gil, and I. Monreal. Increased serum concentrations of procollagen peptides in essential-hypertension - relation to cardiac alterations. *Circulation*, 91 (5):1450–1456, March 1995.

N. J. B. Driessen, G. W. M. Peters, J. M. Huyghe, C. V. C. Bouten, and F. P. T. Baaijens. Remodelling of continuously distributed collagen fibres in soft connective tissues. *J Biomech*, 36(8):1151–1158, August 2003.

J. F. Eberth, N. Popovic, V. C. Gresham, E. Wilson, and J. D. Humphrey. Time course of carotid artery growth and remodeling in response to altered pulsatility. *Am J Physiol-Heart C*, 299(6): H1875–H1883, December 2010.

J. F. Eberth, L. Cardamone, and J. D. Humphrey. Evolving biaxial mechanical properties of mouse carotid arteries in hypertension. *J Biomech*, 44(14):2532–2537, September 2011.

A. Einstein. The motion of elements suspended in static liquids as claimed in the molecular kinetic theory of heat. *Annalen Der Physik*, 17(8):549–560, July 1905.

F. Feihl, L. Liaudet, B. I. Levy, and B. Waeber. Hypertension and microvascular remodelling. *Cardiovas Res*, 78(2):274–285, May 2008.

A Fick. On liquid diffusion. *Phil. Mag*, 10:30–39, 1855.

C. A. Figueroa, S. Baek, C. A. Taylor, and J. D. Humphrey. A computational framework for fluid-solid-growth modeling in cardiovascular simulations. *Computer Methods In Applied Mechanics and Engineering*, 198(45-46):3583–3602, 2009.

M. Flamant, S. Placier, C. Dubroca, B. Esposito, I. Lopes, C. Chatziantoniou, A. Tedgui, J. C. Dussaule, and S. Lehoux. Role of matrix metalloproteinases in early hypertensive vascular remodeling. *Hypertension*, 50(1):212–218, July 2007.

P. J. Flory. Thermodynamic relations for high elastic materials. *T Faraday Soc*, 57:829–838, 1961.

Z. S. Galis and J. J. Khatri. Matrix metalloproteinases in vascular remodeling and atherogenesis - the good, the bad, and the ugly. *Circ Res*, 90(3):251–262, February 2002.

Z. S. Galis, M. Muszynski, G. K. Sukhova, E. Simonmorrisey, E. N. Unemori, M. W. Lark, E. Amento, and P. Libby. Cytokine-stimulated human vascular smooth-muscle cells synthesize a complement of enzymes required for extracellular-matrix digestion. *Circ Res*, 75(1):181–189, July 1994.

A. Garcia. *Experimental and numerical framework for modelling vascular diseases and medical devices*. PhD thesis, University of Zaragoza, 2012.

S. Glagov, C. Zarins, D. P. Giddens, and D. N. Ku. Hemodynamics and atherosclerosis - insights and perspectives gained from studies of human arteries. *Arch Pathol Lab Med*, 112(10):1018–1031, October 1988.

V. Gupta and K. J. Grande-Allen. Effects of static and cyclic loading in regulating extracellular matrix synthesis by cardiovascular cells. *Cardiovas Res*, 72(3):375–383, December 2006.

M. A. Hajdu and G. L. Baumbach. Mechanics of large and small cerebral-arteries in chronic hypertension. *Am J Physiol*, 266(3):H1027–H1033, March 1994.

P. Hamet, V. Hadrava, U. Kruppa, and J. Tremblay. Transforming growth-factor beta-1 expression and effect in aortic smooth-muscle cells from spontaneously hypertensive rats. *Hypertension*, 17 (6):896–901, June 1991.

DOI: 10.1002/cnm

T. P. Harrigan and J. J. Hamilton. An analytical and numerical study of the stability of bone remodeling theories - dependence on microstructural stimulus. *J Biomech*, 25(5):477–488, May 1992.

K. Hayashi, H. Handa, S. Nagasawa, A. Okumura, and K. Moritake. Stiffness and elastic behavior of human intracranial and extracranial arteries. *J Biomech*, 13(2):175–179, 1980.

G. A. Holzapfel. *Nonlinear Solid Mechanics: A Continuum Approach for Engineering*. John Wiley & Sons, 2000.

J. J. Hu, S. Baek, and J. D. Humphrey. Stress-strain behavior of the passive basilar artery in normotension and hypertension. *J Biomech*, 40(11):2559–2563, 2007a.

J.-J. Hu, T. W. Fossum, M. W. Miller, H. Xu, J.-C. Liu, and J. D. Humphrey. Biomechanics of the porcine basilar artery in hypertension. *Ann Biomed Eng*, V35(1):19–29, January 2007b.

J. J. Hu, A. Ambrus, T. W. Fossum, M. W. Miller, J. D. Humphrey, and E. Wilson. Time courses of growth and remodeling of porcine aortic media during hypertension: A quantitative immunohistochemical examination. *J Histochem Cytochem*, 56(4):359–370, April 2008.

K Huang. *Statistical Mechanics*. Wiley, 2 edition, 1987.

Z. J. Huang and J. M. Tarbell. Numerical simulation of mass transfer in porous media of blood vessel walls. *Am J Physiol-Heart C*, 273(1):H464–H477, July 1997.

J.D. Humphrey and K.R. Rajagopal. A constrained mixture model for arterial adaptations to a sustained step change in blood flow. *Biomech Model Mechan*, V2(2):109–126, November 2003.

B. Jani and C. Rajkumar. Ageing and vascular ageing. *Postgraduate Medical Journal*, 82(968): 357–362, June 2006.

W. S. Kim and J. M. Tarbell. Macromolecular transport through the deformable porous-media of an artery wall. *J Biomech Eng-T ASME*, 116(2):156–163, May 1994.

E. Kuhl. *Theory and numerics of open system continuum thermodynamics - spatial and material settings* -. PhD thesis, University of Kaiserslautern, 2003.

E. Kuhl and P. Steinmann. Theory and numerics of geometrically non-linear open system mechanics. *Int J Numer Meth Eng*, 58(11):1593–1615, 2003.

E. Kuhl, A. Menzel, and P. Steinmann. Computational modeling of growth. *Comput Mech*, V32(1): 71–88, September 2003.

E. Kuhl, K. Garikipati, E. M. Arruda, and K. Grosh. Remodeling of biological tissue: Mechanically induced reorientation of a transversely isotropic chain network. *J Mech Phys Solids*, 53(7):1552–1573, July 2005.

C. Laviades, N. Varo, J. Fernandez, G. Mayor, M. J. Gil, I. Monreal, and J. Diez. Abnormalities of the extracellular degradation of collagen type i in essential hypertension. *Circulation*, 98(6): 535–540, August 1998.

J. R. Levick. Flow through interstitium and other fibrous matrices. *Q J Exp Physiol CMS*, 72(4): 409–438, October 1987.

Y. S. J. Li, J. H. Haga, and S. Chien. Molecular basis of the effects of shear stress on vascular endothelial cells. *J Biomech*, 38(10):1949–1971, October 2005.

A. J. Lusis. Atherosclerosis. *Nature*, 407(6801):233–241, September 2000.

E. Maher and A. Creane and S. Sultan and N. Hynes and C. Lally and D.J. Kelly. Inelasticity of Human Carotid Atherosclerotic Plaque. *Ann Biomed Eng*, V(35):19–29, 2007.

DOI: 10.1002/cnm

J. E. Marsden and T. J. R. Hughes. *Mathematical Foundations of Elasticity*. Dover Publications, 1994.

J. Massague. How cells read tgf-beta signals. *Nat Rev Mol Cell Bio*, 1(3):169–178, December 2000.

J. Massague. Tgf beta in cancer. *Cell*, 134(2):215–230, July 2008.

J. Massague, S. W. Blain, and R. S. Lo. Tgf beta signaling in growth control, cancer, and heritable disorders. *Cell*, 103(2):295–309, October 2000.

J. C. Maxwell. *Theory of heat*. Westport, Conn., Greenwood Press, 1871.

M. McNulty, A. Mahmud, P. Spiers, and J. Feely. Collagen type-i degradation is related to arterial stiffness in hypertensive and normotensive subjects. *Journal of Human Hypertension*, 20(11): 867–873, November 2006.

H. Nagase and J. F. Woessner. Matrix metalloproteinases. *Journal of Biological Chemistry*, 274 (31):21491–21494, July 1999.

Kelly D.J. Nagel, T. Remodelling of collagen fibre transition stretch and angular distribution in soft biological tissues and cell-seeded hydrogels. *Biomech Model Mechan*, In Press.

C. J. O'Callaghan and B. Williams. Mechanical strain-induced extracellular matrix production by human vascular smooth muscle cells - role of tgf-beta 1. *Hypertension*, 36(3):319–324, September 2000.

M. K. O'Connell, S. Murthy, S. Phan, C. Xu, J. Buchanan, R. Spilker, R. L. Dalman, C. K. Zarins, W. Denk, and C. A. Taylor. The three-dimensional micro- and nanostructure of the aortic medial lamellar unit measured using 3d confocal and electron microscopy imaging. *Matrix Biol*, 27(3): 171–181, April 2008.

A. G. Ogston, B. N. Preston, J. D. Wells, A. G. Ogston, B. N. Preston, J. M. Snowden, and J. D. Wells. Transport of compact particles through solutions of chain-polymers. *P Roy Soc Lond A Mat*, 333(1594):297–316, 1973.

G. K. Owens. Control of hypertrophic versus hyperplastic growth of vascular smooth-muscle cells. *Am J Physiol*, 257(6):H1755–H1765, December 1989.

G. K. Owens. Regulation of differentiation of vascular smooth-muscle cells. *Physiol Rev*, 75(3): 487–517, July 1995.

G. K. Owens, P. S. Rabinovitch, and S. M. Schwartz. Smooth-muscle cell hypertrophy versus hyperplasia in hypertension. *P Natl Acad Sci-biol*, 78(12):7759–7763, 1981.

J. Philibert. One and a half century of diffusion : Fick , einstein , before and beyond. *Mat Sci+*, 4 (6):1–19, 2006.

E. Porreca, O. DiFebbo, G. Mincione, M. Reale, G. Baccante, M. D. Guglielmi, F. Cuccurullo, and G. Colletta. Increased transforming growth factor-beta production and gene expression by peripheral blood monocytes of hypertensive patients. *Hypertension*, 30(1):134–139, July 1997.

W. F. Pritchard, P. F. Davies, Z. Derafshi, D. C. Polacek, R. C. Tsao, R. O. Dull, S. A. Jones, and D. P. Giddens. Effects of wall shear stress and fluid recirculation on the localization of circulating monocytes in a three-dimensional flow model. *J Biomech*, 28(12):1459–1469, December 1995.

E. W. Raines. Pdgf and cardiovascular disease. *Cytokine Growth F R*, 15(4):237–254, August 2004.

DOI: 10.1002/cnm

A. B. Roberts, M. B. Sporn, R. K. Assoian, J. M. Smith, N. S. Roche, L. M. Wakefield, U. I. Heine, L. A. Liotta, V. Falanga, J. H. Kehrl, and A. S. Fauci. Transforming growth-factor type-beta - rapid induction of fibrosis and angiogenesis invivo and stimulation of collagen formation invitro. *Proceedings of the National Academy of Sciences of the United States of America*, 83(12):4167–4171, June 1986.

P. Saez, V. Alastrue, E. Pena, M. Doblare, and M. A. Martinez. Anisotropic microsphere-based approach to damage in soft fibered tissue. *Biomechanics and Modeling In Mechanobiology*, 11 (5):595–608, May 2012a.

P. Saez, E. Pena, M.A. Martinez, and E. Kuhl. Mathematical modeling of collagen turnover in biological tissue. *J Math Bio.*, 2012b.

P. Saez, E. Pena, M. A. Martinez, and E. Kuhl. Mathematical modeling of collagen turnover in biological tissue. *Journal of Mathematical Biology*, 67(6-7):1765–1793, December 2013.

P. Saez, E. Pena, and M. A. Martinez. A structural approach including the behavior of collagen cross-links to model patient-specific human carotid arteries. *Annals of Biomedical Engineering*, 42(6):1158–1169, June 2014.

R. Sarzani, P. Brecher, and A. V. Chobanian. Growth-factor expression in aorta of normotensive and hypertensive rats. *J Clin Invest*, 83(4):1404–1408, April 1989.

B. D. Schaan, A. S. Quadros, R. Sarmento-Leite, G. De Lucca, A. Bender, and M. Bertoluci. 'correction:' serum transforming growth factor beta-1 (tgf-beta-1) levels in diabetic patients are not associated with pre-existent coronary artery disease. *Cardiovasc Diabetol*, 6:19, July 2007.

I. Schofield, R. Malik, A. Izzard, C. Austin, and A. Heagerty. Vascular structural and functional changes in type 2 diabetes mellitus - evidence for the roles of abnormal myogenic responsiveness and dyslipidemia. *Circulation*, 106(24):3037–3043, December 2002.

G. Sommer and G. A. Holzapfel. 3d constitutive modeling of the biaxial mechanical response of intact and layer-dissected human carotid arteries. *J Mech Behav Biomed*, 5(1):116–128, January 2012.

D. A. Stakos, D. N. Tziakas, G. K. Chalikias, K. Mitrousi, C. Tsigalou, and H. Boudoulas. Associations between collagen synthesis and degradation and aortic function in arterial hypertension. *American Journal of Hypertension*, 23(5):488–494, May 2010.

B. H. Strauss and M. Rabinovitch. Adventitial fibroblasts - defining a role in vessel wall remodeling. *Am J Resp Cell Mol*, 22(1):1–3, January 2000.

B. E. Sumpio, A. J. Banes, W. G. Link, and G. Johnson. Enhanced collagen production by smooth-muscle cells during repetitive mechanical stretching. *AArch Surg*, 123(10):1233–1236, October 1988.

Pablo Saez, Estefania Pena, Miguel Angel Martinez, and Ellen Kuhl. Computational modeling of hypertensive growth in the human carotid artery. *Computational Mechanics*, 53(6):1183–1196, 2014.

S. Tada and J. M. Tarbell. Flow through internal elastic lamina affects shear stress on smooth muscle cells (3d simulations). *Am J Physiol-Heart C*, 282(2):H576–H584, February 2002.

J. Tan, Q. Hua, M. R. Xing, J. Wen, R. K. Liu, and Z. Yang. Impact of the metalloproteinase-9/tissue inhibitor of metalloproteinase-1 system on large arterial stiffness in patients with essential hypertension. *Hypertension Research*, 30(10):959–963, October 2007.

J. M. Tarbell. Mass transport in arteries and the localization of atherosclerosis. *Annu Rev Biomed Eng*, 5:79–118, 2003.

DOI: 10.1002/cnm

C. Truesdell and W. Noll. *The Non-Linear Field Theories of Mechanics*. Springer-Verlag, 3rd edition, 2004.

D. M. Wang and J. M. Tarbell. Modeling interstitial flow in an artery wall allows estimation of wall shear-stress on smooth-muscle cells. *J Biomech Eng-T ASME*, 117(3):358–363, August 1995.

J. Welty, C. E. Wicks, G. L. Rorrer, and R. E. Wilson. *Fundamentals of Momentum, Heat and Mass Transfer*. John Wiley & Sons, 2008.

J. Wiener, A. V. Loud, F. GiacomelliI, and P. Anversa. Morphometric analysis of hypertension-induced hypertrophy of rat thoracic aorta. *Am J Pathol*, 88(3):619–633, 1977.

S. M. WojtowiczPraga, R. B. Dickson, and M. J. Hawkins. Matrix metalloproteinase inhibitors. *Invest New Drug*, 15(1):61–75, 1997.

Harvey Wolinsky. Effects of hypertension and its reversal on the thoracic aorta of male and female rats: Morphological and chemical studies. *Circ Res*, 28(6):622–637, 1971.

J. L. Wrana, L. Attisano, R. Wieser, F. Ventura, and J. Massague. Mechanism of activation of the tgf-beta receptor. *Nature*, 370(6488):341–347, August 1994.

L. Yang. *Mechanical properties of collagen fibrils and elastic fibers explored by AFM*. PhD thesis, Universityof Twente, 2008.

Yasmin, C. M. McEniery, S. Wallace, Z. Dakham, P. Pusalkar, K. Maki-Petaja, M. J. Ashby, J. R. Cockcroft, and I. B. Wilkinson. Matrix metalloproteinase-9 (mmp-9), mmp-2, and serum elastase activity are associated with systolic hypertension and arterial stiffness (vol 25, pg 372, 2005). *Arteriosclerosis Thrombosis and Vascular Biology*, 25(4):875–875, April 2005.

DOI: 10.1002/cnm